**Cell, Volume *126***

# Supplemental Data

# Rules for NLS Recognition by Karyopherinβ2 and Mechanism of Substrate Release by RanGTP

**Brittany J. Lee, Ahmet E. Cansizoglu, Katherine E. Süel, Thomas H. Louis, Zichao Zhang, and Yuh Min Chook**

## HEAT Repeat Nomenclature

Individual helices are named according to their position in the HEAT repeat such that the A helix of HEAT repeat 1 is abbreviated to H1A. HEAT repeat 1 spans residues 1-40 and includes the first two helices (Chook et al., 2002). We note that the first and last pairs of helices in the originally reported Kapβ2-Ran structure were not labeled as HEAT repeats due to structural deviations compared to other repeats (Chook and Blobel, 1999). However, they were later renamed to repeats H1 and H20 to conform to a standard Kapβ HEAT numbering system (Bayliss et al., 2000; Chook et al., 2002; Cingolani et al., 1999; Vetter et al., 1999).

Table S1.

Kap β2-M9NLS Complex

Data Collection:

| Native: | | Selenomethionine: | |
|---|---|---|---|
| Resolution 100.00 - 3.05 Å | | Resolution 100.00 – 3.30 Å | |
| Space group C2 | | Space group C2 | |
| a=152.01 Å, b=154.09 Å, c=141.67 Å, β=91.75° | | a=155.65 Å, b=154.59 Å, c=141.56 Å, β=91.56° | |
| [a]$R_{sym}$ | 0.055 (0.429)[b] | [a]$R_{sym}$ | 0.103 (0.500)[b] |
| I/σ | 24.7 (2.0)[b] | I/σ | 21.5 (2.1)[b] |
| Redundancy | 4.6 (4.1)[b] | Redundancy | 4.9 (4.7)[b] |
| Completeness | 99.0% (92.8%)[b] | Completeness | 98.5% (91.5%)[b] |

Refinement:

Resolution 100.00 - 3.05 Å

[c]$R_{factor}$ = 0.242 $R_{free}$ = 0.272

rmsd from ideal bond lengths 0.0074 Å

rmsd from ideal bond angles 1.136°

Ramachandran Plot: 90.4% in most favored regions, 9.6% in allowed regions

Model:

| | Residues | Average B factor |
|---|---|---|
| Complex 1: | | |
| Kap β2 Chain A | 6-36, 44-77, 80-319, 368-890 | 72.7 Å$^2$ |
| M9NLS Chain C | 263-289 | 81.9 Å$^2$ |
| Complex 2: | | |
| Kap β2 Chain B | 6-36, 44-55, 59-75, 80-319, 368-890 | 74.4 Å$^2$ |
| M9NLS Chain D | 266-289 | 77.6 Å$^2$ |

[a]Rsym = $\sum_h \sum_i | (I_i(h) — \langle I(h) \rangle | / \sum_h \sum_i I_i(h)$; $I_i(h)$ is the i-th measurement of reflection h and $\langle I(h) \rangle$ is the weighted mean of all measurements of h.

[b]Values in parentheses are calculated for data in the highest resolution shell

[c]R factor = $\sum_h | |F_{obs}(h)| - |F_{calc}(h)| | / \sum_h F_{obs}(h) |$; $R_{free}$ is calculated with 10% of the data.

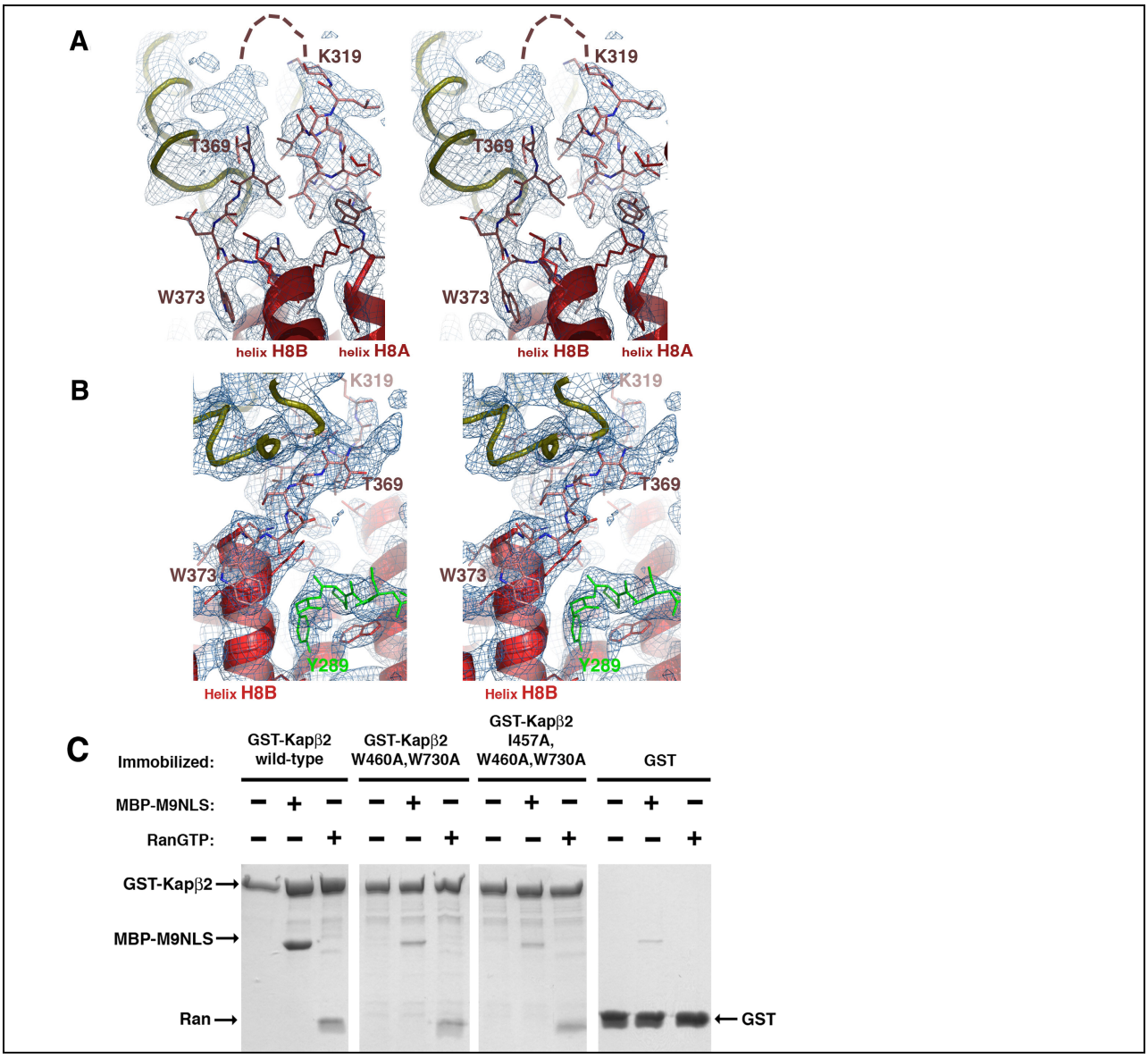


Figure S1. (A) Stereo diagram of the 2Fo-Fc map (1.0 σ, blue mesh) drawn at Kapβ2 (red) HEAT repeat 8, showing H8 loop residues 312-319 connecting to H8A and residues 369–374 to H8B. A neighboring Kapβ2 in the crystal is shown as a yellow ribbon. Red dashes represent the disordered connection between loop residues 319 and 369. (B) similar to A, rotated ~90° about the vertical axis. M9NLS is in green. (C) Binding studies of MBP-M9NLS and immobilized Kapβ2 mutants. Control experiments were also performed using immobilized Kapβ2 proteins and RanGTP.

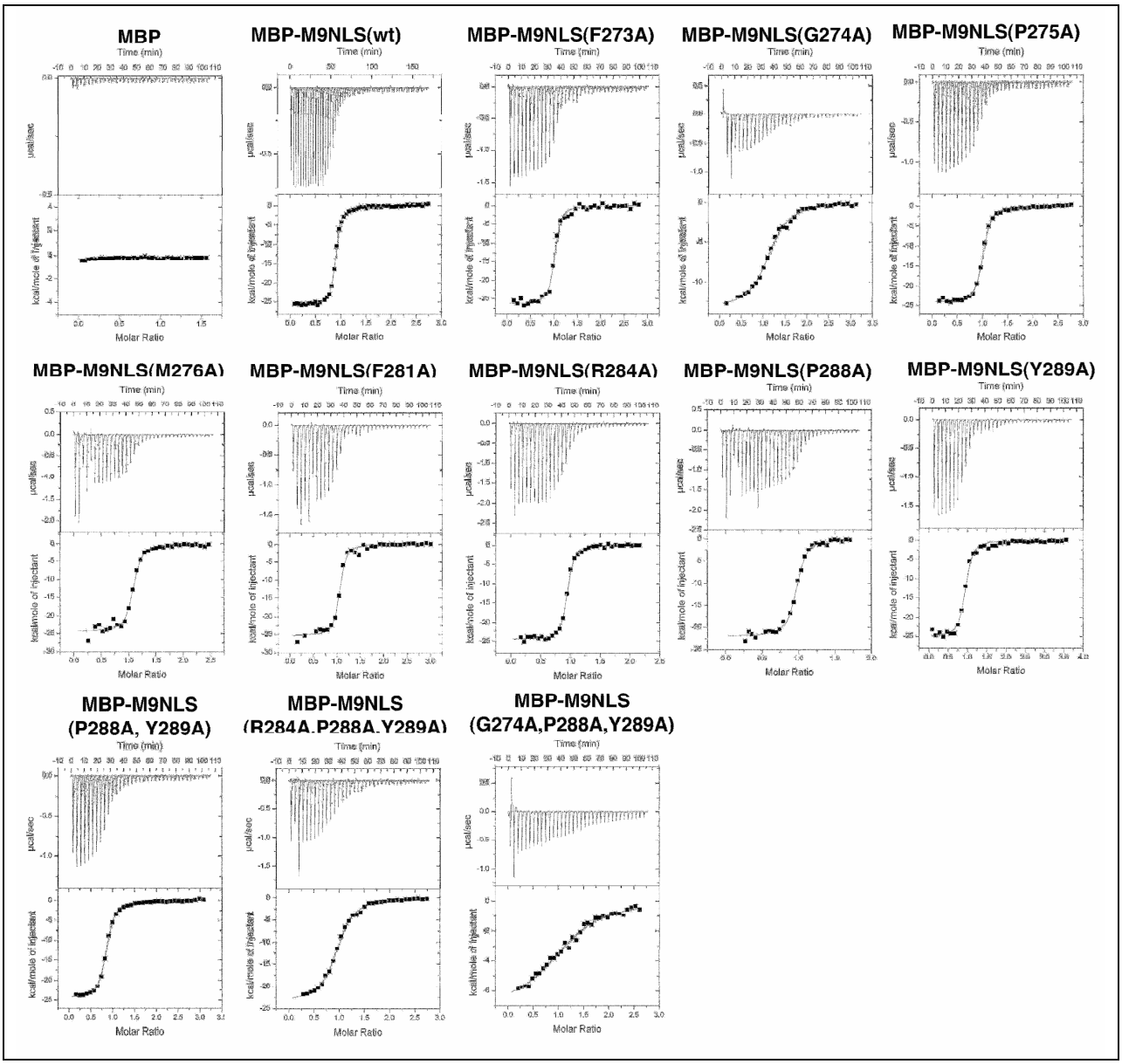


Figure S2. ITC profiles of MBP, MBP fusions of wild type M9NLS and various alanine mutants interacting with full length Kapβ2. Nonlinear least squares fits to the single binding site model were use to fit the ITC profiles (closed squares).

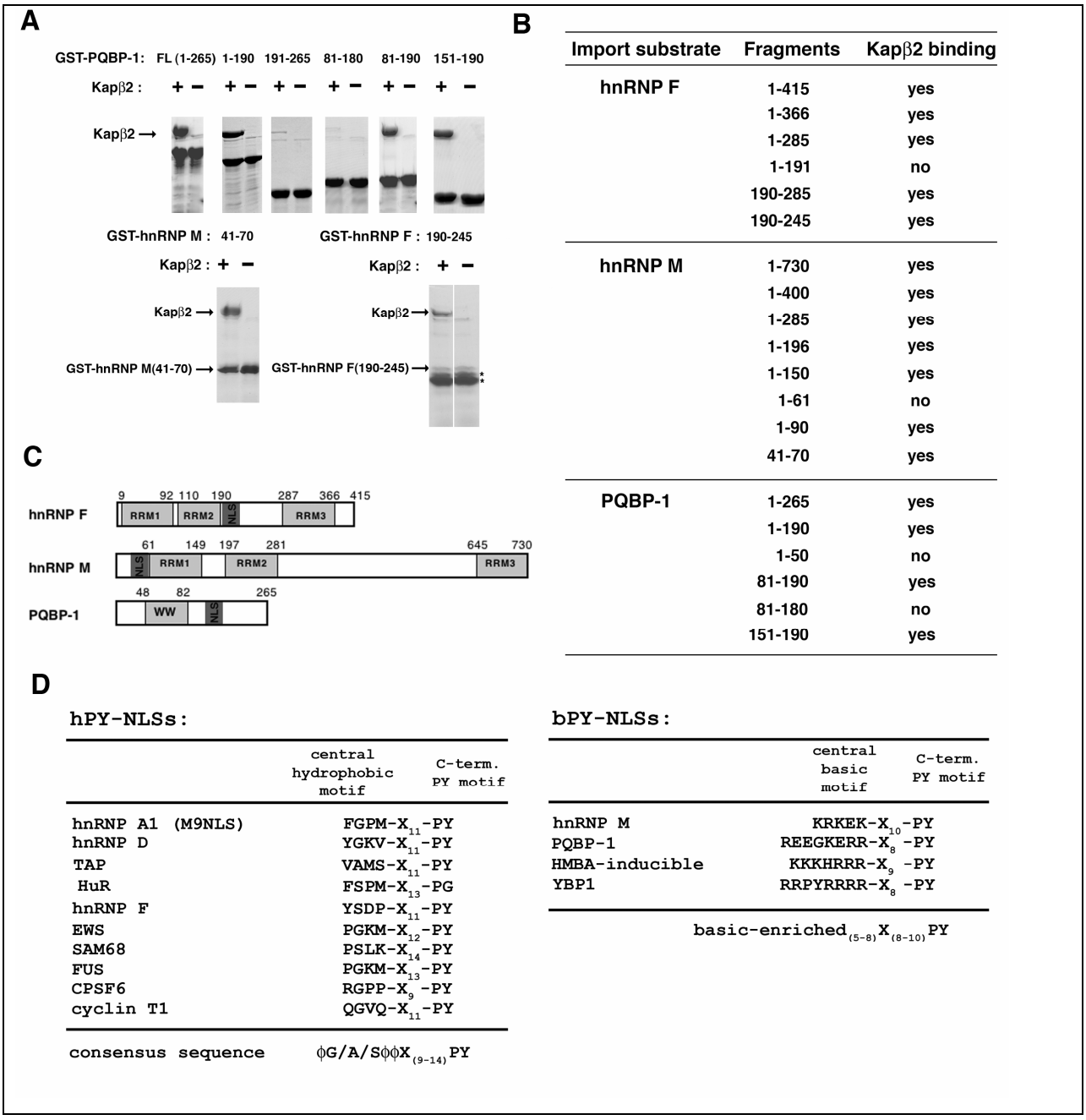


| Import substrate | Fragments | Kapβ2 binding |
|---|---|---|
| hnRNP F | 1-415 | yes |
| | 1-366 | yes |
| | 1-285 | yes |
| | 1-191 | no |
| | 190-285 | yes |
| | 190-245 | yes |
| hnRNP M | 1-730 | yes |
| | 1-400 | yes |
| | 1-285 | yes |
| | 1-196 | yes |
| | 1-150 | yes |
| | 1-61 | no |
| | 1-90 | yes |
| | 41-70 | yes |
| PQBP-1 | 1-265 | yes |
| | 1-190 | yes |
| | 1-50 | no |
| | 81-190 | yes |
| | 81-180 | no |
| | 151-190 | yes |

| | central hydrophobic motif | C-term. PY motif |
|---|---|---|
| hnRNP A1 (M9NLS) | FGPM-$X_{11}$-PY | |
| hnRNP D | YGKV-$X_{11}$-PY | |
| TAP | VAMS-$X_{11}$-PY | |
| HuR | FSPM-$X_{13}$-PG | |
| hnRNP F | YSDP-$X_{11}$-PY | |
| EWS | PGKM-$X_{12}$-PY | |
| SAM68 | PSLK-$X_{14}$-PY | |
| FUS | PGKM-$X_{13}$-PY | |
| CPSF6 | RGPP-$X_{9}$-PY | |
| cyclin T1 | QGVQ-$X_{11}$-PY | |
| consensus sequence | $\phi$G/A/S$\phi\phi$X$_{(9-14)}$PY | |

| | central basic motif | C-term. PY motif |
|---|---|---|
| hnRNP M | KRKEK-$X_{10}$-PY | |
| PQBP-1 | REEGKERR-$X_{8}$-PY | |
| HMBA-inducible | KKKHRRR-$X_{9}$-PY | |
| YBP1 | RRPYRRRR-$X_{8}$-PY | |
| basic-enriched$_{(5-8)}$X$_{(8-10)}$PY | | |

Figure S3. (A) Binding assays of Kapβ2 and immobilized deletion mutants of PQBP-1, hnRNP M, and F. Degraded fragments of the substrates are labeled with asterisks. (B) Summary of all binding assays to map NLSs of PQBP-1, hnRNP M, and F. (C) Location of newly characterized NLSs of PQBP-1, hnRNP M, and F. RNA binding domains (RRMs) and WW-domain are shaded light gray and the NLSs are shaded dark gray. (D) Summary of the central hydrophobic and basic motifs of the PY-NLSs.

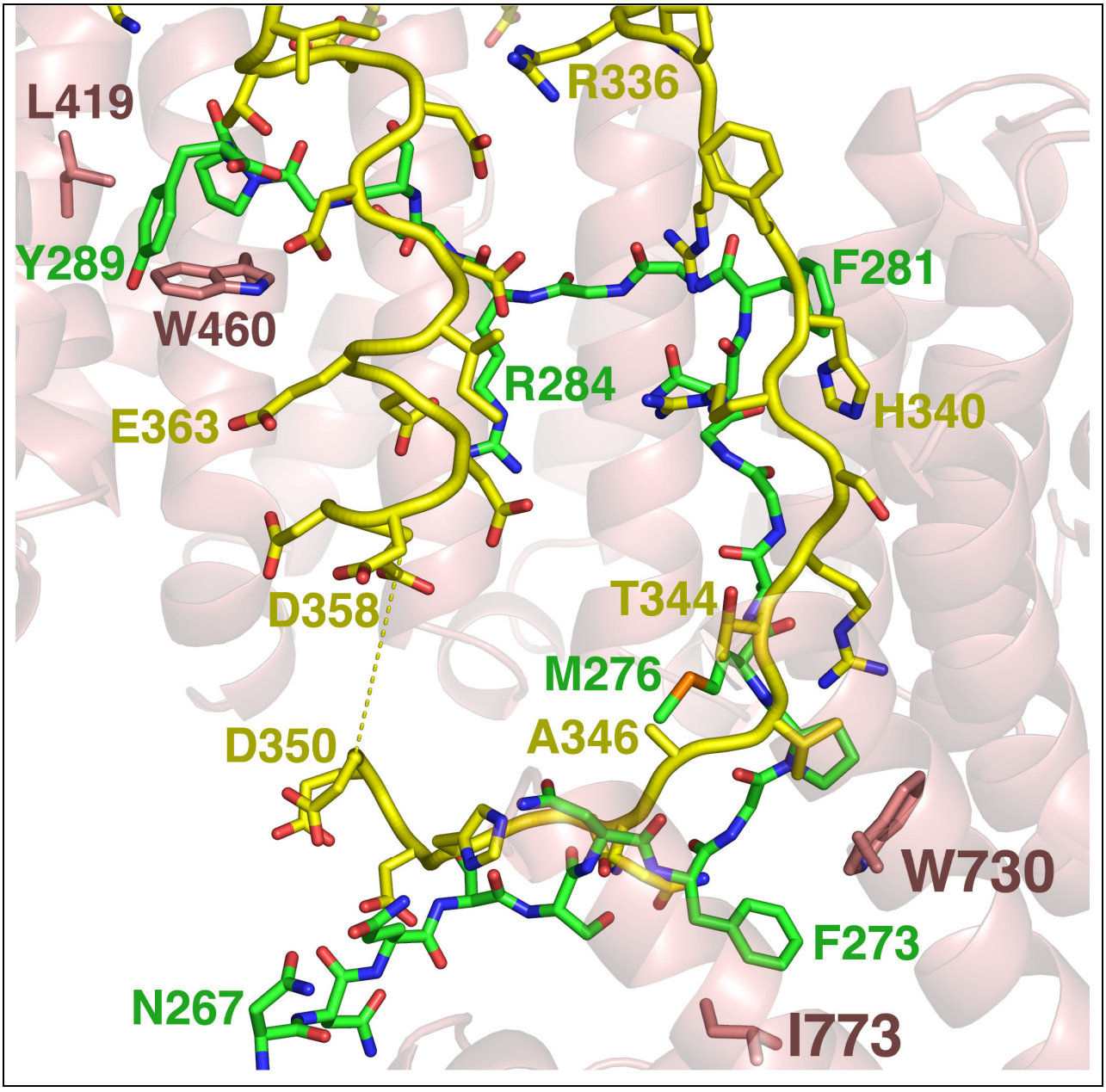


Figure S4. Superposition of the Kapβ2-M9NLS and Kapβ2-Ran complexes, showing the spatial overlap between the Kapβ2 H8 loop in the Ran state (yellow) and M9NLS (green).

## References

Bayliss, R., Littlewood, T., and Stewart, M. (2000). Structural basis for the interaction between FxFG nucleoporin repeats and importin-beta in nuclear trafficking. Cell 102, 99–108.

Chook, Y., and Blobel, G. (1999). Structure of the nuclear transport complex karyopherin-beta2-Ran.GppNHp. Nature 399, 230–237.

Cingolani, G., Petosa, C., Weis, K., and Muller, C.W. (1999). Structure of importin-beta bound to the IBB domain of importin-alpha. Nature 399, 221–229.

Vetter, I.R., Arndt, A., Kutay, U., Gorlich, D., and Wittinghofer, A. (1999). Structural view of the Ran-Importin beta interaction at 2.3 A resolution. Cell 97, 635–646.